Heliyon 9 (2023) e18704

Contents lists available at ScienceDirect

Heliyon

journal homepage: www.cell.com/heliyon

Detection of breast cancer cells by a near-infrared fluorescent probe targeting mitochondrial viscosity

Yu Shi [a,1], Junjun Liu [a,1], Yingying Liu [b,1], Hong Quan [a], Bo Li [a], Haili Lu [a], Hanzhi Ding [a], Zuoren Yu [c,**], Jing Han [a,*]

[a] Department of Breast Cancer, Shanghai East Hospital, Tongji University School of Medicine, Shanghai 200120, China
[b] Department of Physiology and Pathophysiology, Health Science Center, Peking University, Beijing 100191, China
[c] Research Center for Translational Medicine, Shanghai East Hospital, Tongji University School of Medicine, Shanghai 200120, China

ARTICLE INFO

Keywords:
Near-infrared
Viscosity
Mitochondria
Breast cancer

ABSTRACT

Monitoring abnormal viscosity in biological systems is important for basic research and clinical applications. Fluorescence imaging technology is adaptable for the visualization of tumor tissues due to its comprehensive features. However, fluorescence detection of intracellular viscosity in clinical samples remains challenging. We developed a promising near-infrared fluorescent probe, M556, for viscosity measurement. M556, which targets mitochondria, was successfully applied to monitor the mitochondrial viscosity in living cells. Furthermore, M556 was demonstrated to effectively discriminate tumors from normal tissues in a mouse tumor model and in clinical specimens from breast cancer patients, thus indicating the potential perioperative use of this probe by clinicians to assist with biopsy procedures.

1. Introduction

Breast cancer is one of the most common carcinomas worldwide, and surgery is the prominent treatment [1]. The detection of the tumor margin is extremely vital in breast-conserving surgery, and insufficient tumor removal may affect the local recurrence rate. Once the cancer becomes recurrent, the patient might need another operation and shoulder more risks in terms of physical, mental, and economic outcomes [2]. Rapid frozen pathologic examination after tumor resection is the main method to examine the margin of the tumor during an operation [3]; however, this method has some defects, such as a lower accuracy compared to the time-consuming routine approach [4]. Therefore, surgeons need a direct and efficient biomedical imaging tool to examine whether the tissue is invaded by cancer cells.

Modern biomedical fluorescence imaging technology is an indispensable tool in clinical diagnosis and treatment evaluation, by which noninvasive and specialized observation of pathological and physiological events related to human diseases can be conducted *in vivo* [5–7]. In recent years, fluorescence imaging with near-infrared (NIR) wavelengths has gradually been applied by clinicians as a visualization technique because of its unique advantages [8–11].

Probes based on NIR fluorescence have many benefits [12,13]. First, NIR fluorescence imaging technology has an enhanced

* Corresponding author.
** Corresponding author.
E-mail addresses: zuoren.yu@tongji.edu.cn (Z. Yu), Kristall1341@foxmail.com (J. Han).
[1] Co-first authors of this article.

https://doi.org/10.1016/j.heliyon.2023.e18704
Received 12 October 2022; Received in revised form 23 July 2023; Accepted 25 July 2023
Available online 26 July 2023

signal-to-noise ratio and sensitivity compared to other methods [14]. Second, NIR light has deeper tissue penetration, and the depth can reach the millimeter level [15]. Third, due to its relatively low energy, NIR light induces less damage to biological samples than other wavelengths of fluorescent light [16]. As a result, the NIR region is often referred to as the "biological window" and has important applications in disease detection and diagnosis [17], drug development [18], and treatment evaluation [19].

An abnormal intracellular viscosity is related to changes of nucleic acids, proteins, and carbohydrates in cells, which affect various biological activities such as protein folding, enzyme catalytic reactions, and membrane fusion [20–22]. The alteration of mitochondrial viscosity is an essential factor and indicator of many diseases and cellular dysfunction, including malignant tumors, atherosclerosis, hypertension, diabetes, and Alzheimer's disease [23–27]. Therefore, it is of great significance to detect the atypical viscosity of mitochondria in living cells for clinical diagnosis and treatment of diseases. Although there are many probes that can be used to measure mitochondrial viscosity [28–33], determining the relationship between disease and viscosity remains difficult due to the lack of a comprehensive understanding of human physiological processes and multiple disease states in animal models. Breast cancer is commonly treated surgically if sentinel lymph node metastasis is present. Therefore, surgeons need a tool that can assist in labeling lymph nodes and rapidly determine if they bear any tumor cells during an operation because common tracers, such as methylene blue, cannot resolve the specificity of tumor-invaded tissue.

Given the above research requirements, in this study, we designed and synthesized an activatable NIR fluorescence probe, M556, in order to identify the aberrant intracellular viscosity that can be considered a biological marker for breast cancer cells. M556 exhibits a fluorescence quenching state under low-viscosity conditions. Conversely, high viscosity triggers the restriction of intramolecular rotation, which leads to an activated fluorescence signal. This probe not only shows good specificity and photostability in viscous solutions, but it also possesses excellent biocompatibility and low cytotoxicity in living cells. Most importantly, we demonstrated that the probe M556 could be used to specifically visualize tumor cells in both *in-vitro* and *in-vivo* models, as well as in clinical breast cancer samples, indicating the potential of this probe for clinical applications.

2. Materials and methods

2.1. Reagents, cell lines, and mice

All chemical reagents and solvents were purchased from Titan Technologies (Shanghai, China), were of analytical reagent grade, and were directly utilized without further purification, unless otherwise stated. ^{1}H NMR and ^{13}C NMR spectra were recorded using a Bruker AV-400 NMR spectrometer. Fluorescence spectra were recorded on a Hitachi F-7000 fluorescence spectrofluorometer (Japan). Ultraviolet–visible (UV–Vis) spectra were obtained on an INESA L6S instrument (Shanghai, China). MDA-MB-231 and MCF-10A cells were purchased from the National Collection of Authenticated Cell Cultures (Shanghai, China). BALB/c nude mice were obtained from Shanghai Model Organisms Center, Inc. (Shanghai, China). All procedures were approved by the Animal Welfare and Ethical Review Committee at Tongji University.

2.2. Synthesis of M556

Compound **1** (for the synthetic route, refer to Ref. [34]) (425 mg, 1.5 mmol), compound **2** (440 mg, 1.5 mmol), and piperidine (100 μL) were dissolved in 10 mL of dry acetonitrile. The mixture was refluxed under a stream of N_2 gas at 85 °C overnight. After the reaction was finished, the solvent was removed under reduced pressure to harvest the crude product, which was further purified by silica gel column chromatography with dichloromethane (DCM)/methanol (40/1, v/v) as the eluent to afford the target product as a green powder (325 mg, 39%). ^{1}H NMR (400 MHz, DMSO-d_6) δ 8.26–8.06 (m, 2H), 7.88 (d, J = 8.4 Hz, 1H), 7.64 (t, J = 7.3 Hz, 1H), 7.51 (t, J = 7.6 Hz, 1H), 7.31 (d, J = 7.5 Hz, 2H), 6.79–6.55 (m, 3H), 3.99 (s, 3H), 3.46 (q, J = 6.9 Hz, 4H), 2.61 (dt, J = 11.3, 5.1 Hz, 4H), 1.86–1.66 (m, 2H), 1.15 (t, J = 6.9 Hz, 6H). ^{13}C NMR (151 MHz, DMSO) δ 167.57, 159.36, 154.88, 150.58, 141.88, 140.67, 133.69, 128.70, 128.28, 126.12, 125.77, 123.13, 122.56, 114.57, 111.63, 111.24, 110.29, 102.10, 95.92, 54.76, 43.93, 34.27, 28.15, 24.34, 20.12, 12.40. HRMS (ESI) calcd for $C_{27}H_{29}N_2OS$ $[M - I]^+$: 429.1996, found: 429.1986.

2.3. Spectrophotometric experiments

M556 was dissolved in dimethyl sulfoxide (DMSO) to prepare a 1 mM stock solution, which was stored at −4 °C. The probe was added to a 2-mL solution consisting of ethanol and glycerol at various ratios. The mixture was sonicated for 5 min and placed at 25 °C for 30 min to eliminate bubbles. The final working concentration of M556 was 10 μM. The UV–Vis absorption spectrum and fluorescence spectrum measurements were carried out in the ethanol-glycerol system. An increase in viscosity can be caused by changing the percentage of glycerol in an ethanol-glycerol solution (from 100% ethanol to 100% glycerol). The maximum absorption wavelength of the probe (720 nm) was set as the excitation wavelength for the fluorescence spectrum measurement. A series of potential interference species, including cysteine, homocysteine, glutathione, NaClO, H_2O_2, bovine serum albumin, $NaHSO_3$, and NaCl in ultrapure water, were prepared to test the selectivity of the probe. To study the effects of various solvents on the emission spectra of the probes, stock solutions of probes were diluted in 2 mL of H_2O, phosphate-buffered saline (PBS), methanol, DCM, DMSO, CH_3CN, tetrahydrofuran (THF), ethanol, and glycerol, respectively.

2.4. Cell culture and cytotoxicity assay

The cytotoxicity of M556 was examined in MDA-MB-231 cells by a cell counting kit-8 (CCK8) assay. Cells were seeded in a 96-well plate with approximately 5000 cells per well and incubated at 37 °C in a humidified atmosphere containing 5% CO_2 for 24 h. M556 was dissolved in DMSO and added to cells to afford different final concentrations (0 μM, 1 μM, 5 μM, 10 μM, 20 μM, and 30 μM) and then incubated for 24 h. After that, 10 μL of CCK8 reagent was added to each well, and the plate was incubated for another 40 min. The absorbance of each sample was measured at 450 nm in a plate reader. The cell viability was determined by a standard CCK8 assay.

2.5. Colocalization experiments of M556 in living cells

The cells were incubated with 2 μM M556 for 30 min, followed by 1 μM Mito-Tracker Green FM, and then 1 × Hoechst 33342 for another 15 min, in sequence. After that, the cells were washed three times with PBS and then imaged. The fluorescence signals of Hoechst 33342 were collected at 430–480 nm with an excitation at 405 nm. The fluorescence signals of the probe M556 were collected at 740–800 nm with an excitation at 720 nm. The fluorescence signals of Mito-Tracker Green FM were collected at 500–550 nm with an excitation at 488 nm.

2.6. Fluorescence imaging in living cells

MDA-MB-231 and MCF-10A cells were incubated with the probe M556 (2 μM) (containing 0.1% DMSO as a cosolvent) for 30 min. Next, the cells were washed three times with PBS, and then 1 mL of PBS was added to observe the fluorescence signal under a confocal microscope. Hoechst 33342 was added to the cells after the probe, and the cells were incubated for 15 min to stain the cell nuclei.

2.7. Establishment and fluorescence imaging of a tumor-bearing mouse model

Six-week-old female BALB/c nude mice were purchased from Shanghai Model Organisms Center, Inc. The experiments were approved by the Animal Ethical Experimentation Committee of Tongji University School of Medicine, Shanghai, PR China. The mice were inoculated with MDA-MB-231 cells, and tumors were obtained after 14 days. The tumor-bearing mice and normal mice were simultaneously utilized for *in-vivo* imaging. The mice were anesthetized, and then M556 (10 μM, 100 μL) was injected into the leg muscle position of the normal mice and tumor-grafted mice hypodermically. Next, the organs (heart, liver, spleen, lung, and kidney) and tumors were isolated from the mice. After washing with PBS (pH 7.4) three times, these isolated organs and tumors were stained with M556 (10 μM). All of the images were taken by an *in-vivo* imaging system.

2.8. Fluorescence imaging of clinical samples

After the clinical specimens were obtained, they were cut to the same size and immediately incubated with M556 solution (10 μM) for 20 min, and then they were washed with PBS three times. Next, fluorescence imaging was performed using an *in-vivo* imaging system. Afterwards, the clinical samples were fixed with 4% paraformaldehyde solution, embedded in paraffin, sliced, and stained with hematoxylin-eosin, followed by microscopic observation and imaging. The study was approved by the Ethics Committee of the East Hospital, Shanghai, PR China.

3. Results and discussion

3.1. Synthesis and characterization of M556

Twisting intramolecular charge transfer (TICT) is a classical strategy for designing fluorescent probes to monitor viscosity. It is a relatively common phenomenon in molecules that consist of an electron donor and acceptor pair linked by a single bond. The mechanism of TICT is to connect the electron donor and the electron acceptor through conjugated bonds, forming a push-pull electron-conjugated system. However, the twist of TICT will cause the change of the energy level difference between the ground state and the excited state, and the energy level difference is related to the rotation angle of the donor and the acceptor. A TICT-based fluorophore is an ideal sensor for detecting features in a microenvironment such as viscosity [35,36].

As shown in Fig. 1, the fluorescent probe M556 was synthesized from two compounds: Compound **1** is a fluorophore containing a diethylamino group as a strong electron donor and a rigid three-ring conjugated system to strengthen the π system, and compound **2** (*N*-methyl-2-methyl benzothiazole salt cation) has an electron-accepting group that can target mitochondria. Due to its excitation and emission wavelengths in the NIR region, M556 can successfully sense the viscosity in tumor tissue and be utilized for the imaging of living systems. The chemical structure of M556 was characterized by ^{1}H NMR, ^{13}C NMR, and high-resolution mass spectrometry (Figures S1–S2 and S4).

3.2. Fluorescence spectral analyses of M556

Glycerol was used as a viscous medium, while ethanol was used as a nonviscous medium. Solutions of the probe (10 mM) under different viscosity conditions were prepared with ethanol/glycerol mixtures as the solvent. The fluorescence spectra were measured

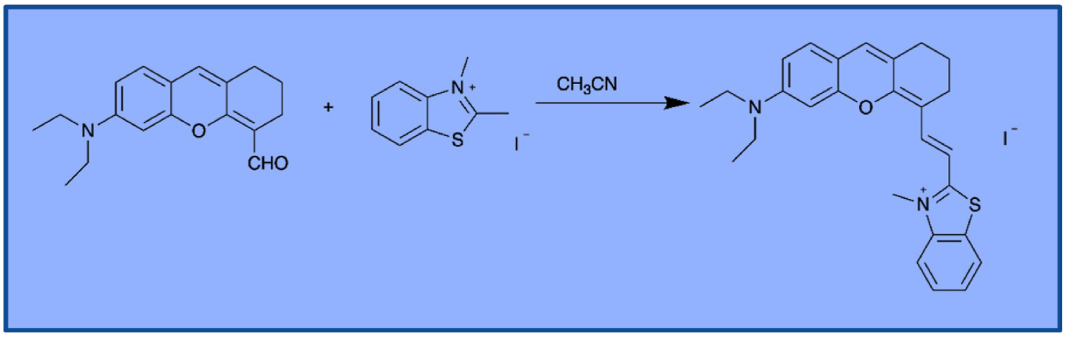

Fig. 1. Synthetic route of M556. The fluorescent probe M556 was synthesized from a fluorophore containing a diethylamino group and a rigid three-ring conjugated system, and *N*-methyl-2-methyl benzothiazole salt cation. The chemical structure of M556 was characterized by ^{1}H NMR, ^{13}C NMR and high-resolution mass spectrometry (Figures S1-S2 and S4).

with an excitation wavelength of 720 nm and a slit of 2 nm.

The effect of viscosity changes on the fluorescence absorption spectra of the probe M556 was studied (Fig. 2). In glycerol, the probe exhibited a weak absorption peak at 720 nm. In contrast, a stronger absorption peak at 720 nm appeared in ethanol (Fig. 2a). By changing the ratio of glycerol to ethanol, a series of mixtures with different viscosities was obtained and then used as testing media to examine the fluorescence spectra of the probe. M556 displayed a weak emission when excited in ethanol (Fig. 2b). With the increase of the v/v ratio of glycerol to ethanol and the corresponding viscosity, the fluorescence intensity of M556 at the emission wavelength was significantly enhanced. A good linear relationship existed between the fluorescence intensity (lg I) and viscosity value (lg η) via the Förster–Hoffmann theory fitting, affording $R^2 = 0.99$ (Fig. 2c). Besides, the Stokes shift was determined as 60 nm ($\lambda_{ex} = 720$ nm and $\lambda_{em} = 780$ nm), which can be a benefit for avoiding the interference of laser signals. In addition, M556 displayed a stable fluorescent signal at 780 nm in 50% glycerol media, which remained almost unchanged over 3600 s (Fig. 2d), suggesting that the probe M556 has good photostability.

Next, the fluorescence spectral profiles of M556 in solvents of various polarities were investigated to assess whether polarity influences the fluorescence of the probe. As shown in Fig. 2e and f, the probe exhibited a strong fluorescence emission in glycerol; in contrast, it showed a much weaker fluorescence in other solvents. This indicates that the probe only responds to viscosity but not polarity, suggesting that the probe could be used to detect viscosity changes in complex microenvironments. These fluorescence

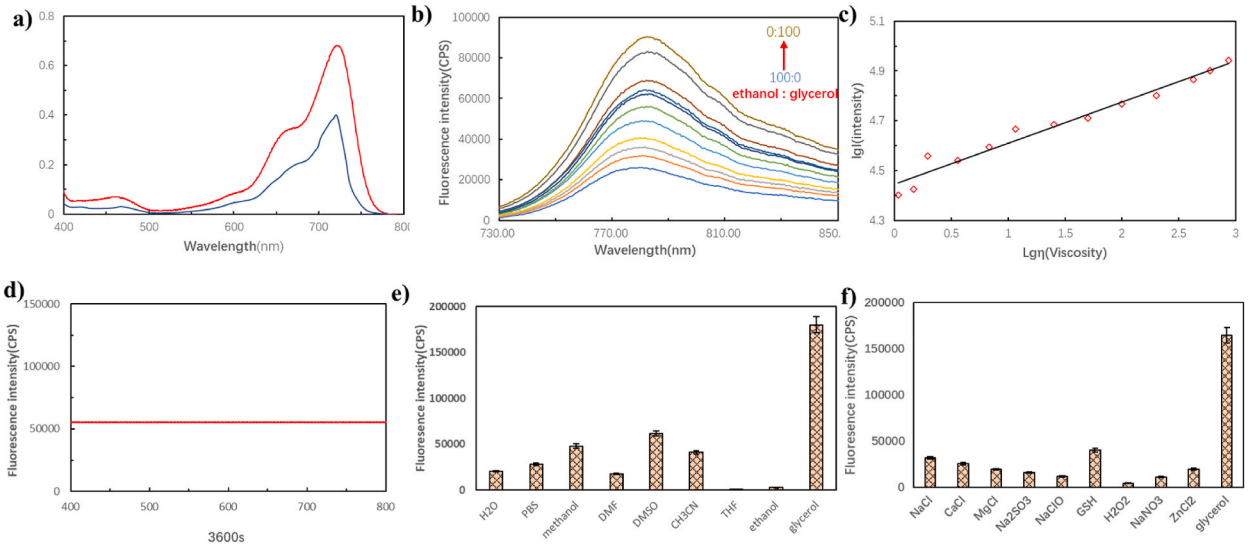

Fig. 2. Fluorescence spectral analyses of M556. UV–Vis absorption of M556 was investigated in ethanol and glycerol, respectively. a) Absorption spectra of the probe M556 (10 μM) in ethanol (red line); b) Fluorescence spectra of M556 (10 μM) in mixed solutions with different ratios of ethanol: glycerol; c) The linearity of lg I (fluorescence intensity) versus lg η (viscosity) of M556 (10 μM) in ethanol-glycerol solution (λex = 720 nm, R^2 = 0.99); d) Time-dependent fluorescence intensity of M556 (10 μM) in 50% glycerol (T = 3600 s); e) Fluorescence emission of the probe M556 in various solvents with different polarities, including H_2O, PBS, methanol, DCM, DMSO, CH_3CN, THF, ethanol, and glycerol (λex = 720 nm, λem = 780 nm). $P < 0.05$ (glycerol vs. other solvents); f) Fluorescence emission of the probe M556 in various solvents with different polarities, including NaCl, CaCl, MgCl, Na_2SO_3, NaClO, GSH, H_2O_2, $NaNO_3$, $ZnCl_2$, and glycerol (λex = 720 nm, λem = 780 nm). $P < 0.05$ (glycerol vs. other solvents). (For interpretation of the references to colour in this figure legend, the reader is referred to the Web version of this article.)

properties demonstrate that M556 is an excellent fluorescent probe for identifying viscosity.

3.3. Application of M556 fluorescence imaging in living cells

Before being applied to living cells, the biological toxicity of M556 was evaluated by CCK8 assays using MDA-MB-231 cells. MDA-MB-231 cells showed more than 80% cell viability at a probe concentration of up to 30 μM and an incubation time as long as 24 h (Fig. S3), suggesting that M556 has a low cytotoxicity under the tested concentrations. Therefore, the probe is biologically safe for subsequent experiments in living cells with a working concentration of 5 μM.

It is generally believed that organic small-molecule probes with positive charges can localize to the mitochondria of living cells. To confirm the subcellular localization of the probe M556, a commercially available fluorescent dye that specifically targets mitochondria (Mito-Tracker Green FM) was employed for this colocalization study. A fluorescence confocal microscope was used to observe cells treated with a mitochondrial marker and M556 (5 μM) together. We noticed that the fluorescent image of M556-labeled mitochondria in the red channel was well overlaid with the image obtained by the Mito-Tracker Green channel (Fig. 3), affording a colocalization coefficient (Pearson's correlation) of 0.92. This result demonstrated that the probe M556 was mainly confined within the mitochondria of living cells.

Next, the fluorescence characteristics of M556 in cancer and normal cells were investigated. MDA-MB-231 cells (cancer cells) and MCF-10A cells (normal cells) were incubated with the probe M556, and confocal fluorescence images were taken under the same imaging conditions. The fluorescence intensity of MDA-MB-231 cells was significantly stronger than that of MCF-10A cells (Fig. 3f). This observation that the viscosity of mitochondria in cancer cells is greater than that in noncancer cells is consistent with the literature [37–40], indicating that the probe M556 can distinguish cancer cells from noncancer cells via different fluorescence intensities.

3.4. Application of M556 to in-vivo fluorescence imaging

We further applied M556 to visualize the abnormal viscosity in a tumor-bearing mouse model. Weak fluorescence was detected in healthy mice; meanwhile, the tumor-bearing mice showed an enhanced fluorescence emission (Fig. 4a), implying that the probe M556 could be used to reveal viscosity variation *in vivo*. Subsequently, the difference in viscosity between normal organs and tumors was also inspected with the probe M556. Weak fluorescence was observed in healthy organs, including the heart, liver, spleen, lung, and kidney,

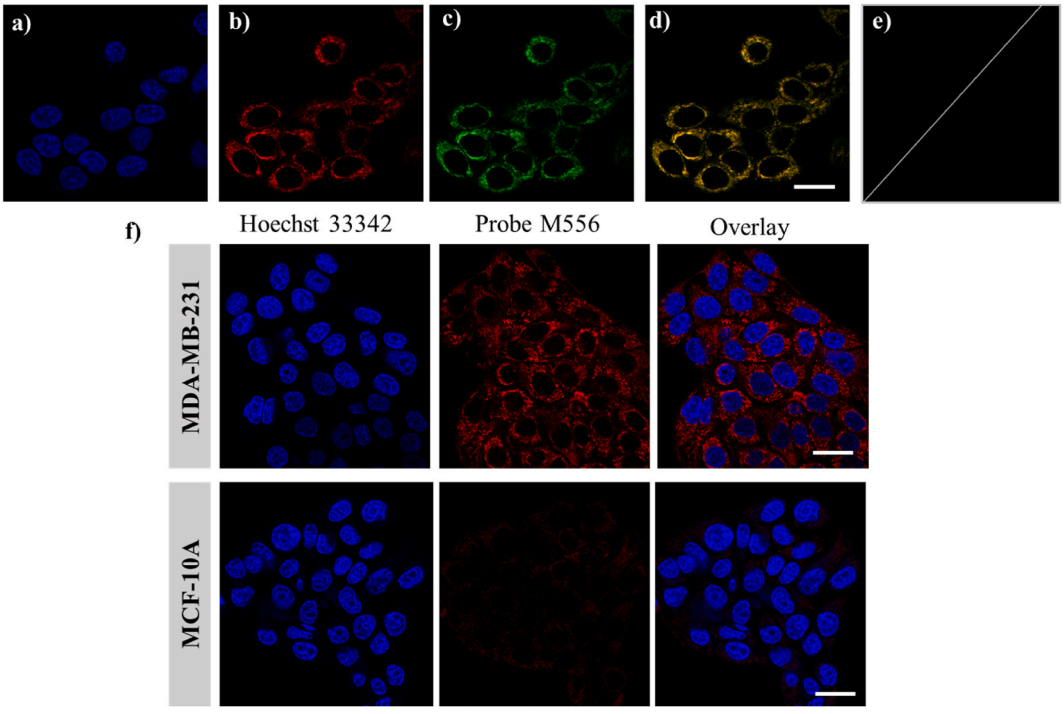

Fig. 3. Subcellular localization of M556 in living cells and measurement of intracellular viscosity with M556. a) Hoechst 33342 (1 × , λex = 405 nm, λem = 430–480 nm) for nuclear staining; b) M556 (5 μM, λex = 720 nm, λem = 740−800 nm); c) Mito-tracker Green (1 μM, λex = 488 nm, λem = 500−550 nm); d) Overlay of (b) and (c) in a bright field. Scale bar = 25 μm; e) The horizonal axis represents M556 and the vertical axis represents Mito-tracker Green. The Pearson's correlation factor was 0.92. f) MDA-MB-231 cells (cancer cells) and MCF-10A cells (normal cells) were treated with M556 (5 μM) for 30 min for fluorescence imaging. The blue channel was the fluorescence signal of the Hoechst 33342 dye, and the red channel was the fluorescence signal of M556. Scale bar = 25 μm. (For interpretation of the references to colour in this figure legend, the reader is referred to the Web version of this article.)

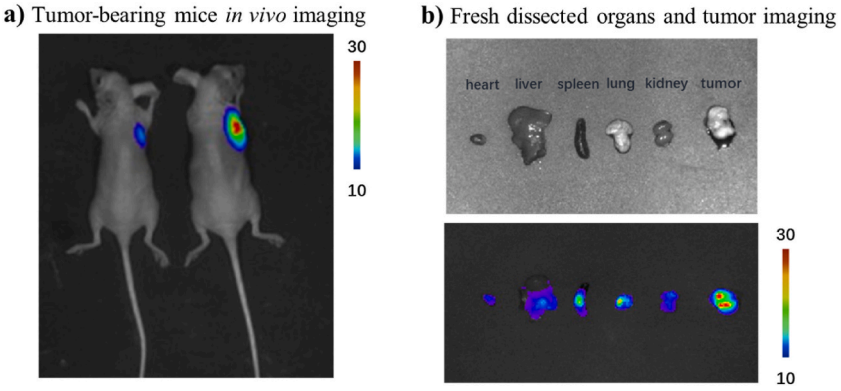

Fig. 4. Fluorescence imaging of M556 *in vivo*. a) A control mouse (on the left) and a tumor-bearing mouse (on the right) inoculated with MDA-MB-231 cells for 14 days were intramuscularly injected with 100 μL of 10 μM M556 and imaged. b) The organs and tumor tissues of the mice were freshly dissected and stained by M556 for imaging.

in contrast to the much more significant fluorescence captured in tumor tissue (Fig. 4b). This finding demonstrates that the viscosity level in a tumor is greater than that in normal organs and that M556 is able to detect viscosity changes *in vivo*.

3.5. Application of M556 in clinical samples

The main purpose of this study was to explore whether the probe M556 can recognize tumor cells in clinical breast cancer samples. Therefore, we obtained two freshly resected tissue samples from breast cancer patients in whom the existence of any tumor was unknown. After the two samples were incubated with M556 for 10 min, fluorescence imaging was immediately performed. These two unknown samples could be distinguished from each other according to the evident difference in fluorescence intensity (Fig. 5a). Afterwards, the sample tissues were fixed with 10% paraformaldehyde and made into paraffin sections, followed by hematoxylin-eosin staining and imaging (Fig. 5b). By comparing the hematoxylin-eosin staining results with the fluorescence imaging results, we confirmed that M556 has the potential in identifying tumors. However, the probe fluorescence intensity from cancer specimen was not uniformly observed, as cancer samples, which contain both normal tissue and tumor tissue with cells in different stages, were not uniform as well. In general, this finding indicates that the probe M556 can effectively distinguish breast tumor tissues from normal tissues in clinical samples and has the potential to assist in clinical surgery.

Today, the era of fluorescence-guided tumor surgery has arrived, and its emergence can aid in the early diagnosis of cancer. Both amputation and surgical operations would benefit from the guidance of accurate tumor resection [5]. With further in-depth studies of targeted activated fluorescent molecular probes, newer and ultrasensitive molecules will be developed and utilized. Activated NIR probes can promote the application of NIR imaging in biomedicine, which is of great importance on the road to precision medicine. Noninvasive NIR image-guided surgery has brought benefits for the treatment of solid tumors, but *in-vivo* imaging penetration is still

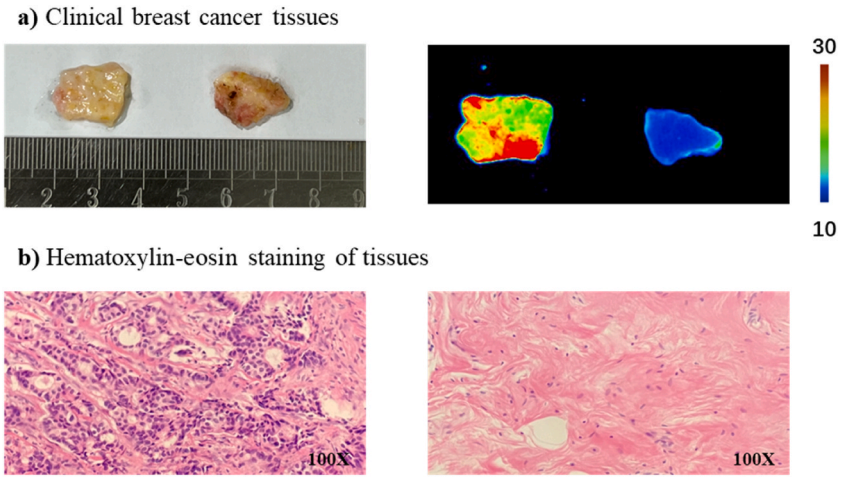

Fig. 5. Fluorescence imaging of M556-treated clinical breast cancer samples. a) Fresh resected tissue samples from a breast cancer patient (left panel), and the fluorescent scanning of these samples after M556 (10 μM) staining for 20 min (right panel). b) Hematoxylin-eosin staining of the paraffin sections (100 ×) from the M556-treated samples shown in a).

limited. Nevertheless, in clinical practice, magnetic resonance imaging and positron emission computed tomography can penetrate deep beneath the skin to identify tumors throughout the body. Therefore, organic integration of NIR fluorescence imaging and other imaging methods can provide better results, finally establishing a multidimensional accurate tumor detection method in order to improve current surgical procedures and the prognosis of cancer patients.

4. Conclusion

We designed and synthesized an activatable molecular probe, M556, which exhibits excellent sensitivity, selectivity, and mitochondria-targeting ability. Notably, M556 was not only successfully applied to detect and visualize viscosity changes in MDA-MB-231 cells, but it was also effective in a tumor-bearing mouse model and clinical specimens. The probe M556 may be used perioperatively by clinicians to assist with biopsy procedures in the future.

Declarations

Author contribution statement

YU SHI: Conceived and designed the experiments; Performed the experiments; Analyzed and interpreted the data; Wrote the paper.
JUNJUN LIU: YINGYING LIU: Performed the experiments.
HONG QUAN: BO LI: Analyzed and interpreted the data.
HAILI LU: HANZHI DING: Contributed reagents, materials, analysis tools or data.
ZUOREN YU: Contributed reagents, materials, analysis tools or data; Wrote the paper.
JING HAN: Conceived and designed the experiments; Wrote the paper.

Data availability statement

Data included in article/supp. material/referenced in article.

Declaration of competing interest

The authors declare that they have no known competing financial interests or personal relationships that could have appeared to influence the work reported in this paper.

Appendix A. Supplementary data

Supplementary data to this article can be found online at https://doi.org/10.1016/j.heliyon.2023.e18704.

References

[1] L. Wilkinson, T. Gathani, Understanding breast cancer as a global health concern, Br. J. Radiol. 95 (1130) (2022), 20211033.
[2] C.C. Park, M. Mitsumori, A. Nixon, et al., Outcome at 8 years after breast-conserving surgery and radiation therapy for invasive breast cancer: influence of margin status and systemic therapy on local recurrence, J. Clin. Oncol. 18 (8) (2000) 1668–1675.
[3] J.M. Jorns, D. Visscher, M. Sabel, et al., Intraoperative frozen section analysis of margins in breast conserving surgery significantly decreases reoperative rates: one-year experience at an ambulatory surgical center, Am. J. Clin. Pathol. 138 (5) (2012) 657–669.
[4] M.G. Giacomelli, T. Yoshitake, L.C. Cahill, et al., Multiscale nonlinear microscopy and widefield white light imaging enables rapid histological imaging of surgical specimen margins, Biomed. Opt Express 9 (5) (2018) 2457–2475.
[5] J.S.D. Mieog, F.B. Achterberg, A. Zlitni, et al., Fundamentals and developments in fluorescence-guided cancer surgery, Nat. Rev. Clin. Oncol. 19 (1) (2022) 9–22.
[6] M.H. Lee, A. Sharma, M.J. Chang, et al., Fluorogenic reaction-based prodrug conjugates as targeted cancer theranostics, Chem. Soc. Rev. 47 (1) (2018) 28–52.
[7] O.T. Okusanya, E.M. Dejesus, J.X. Jiang, et al., Intraoperative molecular imaging can identify lung adenocarcinomas during pulmonary resection, J. Thorac. Cardiovasc. Surg. 150 (1) (2015).
[8] E.R. John, R. Al-Khudairi, H. Ashrafian, et al., Diagnostic accuracy of intraoperative techniques for margin assessment in breast cancer surgery: a meta-analysis, Ann. Surg. 265 (2) (2017) 300–310.
[9] L.D. Lavis, R.T. Raines, Bright building blocks for chemical biology, ACS Chem. Biol. 9 (4) (2014) 855–866.
[10] E.M. Sevick-Muraca, J.C. Rasmussen, Molecular imaging with optics: primer and case for near-infrared fluorescence techniques in personalized medicine, J. Biomed. Opt. 13 (4) (2008), 041303.
[11] A.L. Vahrmeijer, M. Hutteman, J.R. Van der Vorst, et al., Image-guided cancer surgery using near-infrared fluorescence, Nat. Rev. Clin. Oncol. 10 (9) (2013) 507–518.
[12] S. Gioux, H.S. Choi, J.V. Frangioni, Image-guided surgery using invisible near-infrared light: fundamentals of clinical translation, Mol. Imag. 9 (5) (2010) 237–255.
[13] S.Q. He, J. Song, J.L. Qu, et al., Crucial breakthrough of second near-infrared biological window fluorophores: design and synthesis toward multimodal imaging and theranostics, Chem. Soc. Rev. 47 (12) (2018) 4258–4278.
[14] Z. Yang, J. Cao, Y. He, et al., Macro-/micro-environment-sensitive chemosensing and biological imaging, Chem. Soc. Rev. 43 (13) (2014) 4563–4601.
[15] Y.H. Tang, D. Lee, J.L. Wang, et al., Development of fluorescent probes based on protection-deprotection of the key functional groups for biological imaging, Chem. Soc. Rev. 44 (15) (2015) 5003–5015.
[16] J. Liu, C. Chen, S.L. Ji, et al., Long wavelength excitable near-infrared fluorescent nanoparticles with aggregation-induced emission characteristics for image-guided tumor resection, Chem. Sci. 8 (4) (2017) 2782–2789.

[17] J.G. Huang, K.Y. Pu, Near-infrared fluorescent molecular probes for imaging and diagnosis of nephro-urological diseases, Chem. Sci. 12 (10) (2020) 3379–3392.
[18] Y. Miao, C. Gu, Y. Zhu, et al., Recent progress in fluorescence imaging of the near-infrared II window, Chembiochem 19 (24) (2018) 2522–2541.
[19] S. Hameed, Z. Dai, Near-infrared fluorescence probes for surgical navigation, Mater. Today Chem. 10 (2018) 90–103.
[20] G. Ciuffetti, G. Schillaci, R. Lombardini, et al., Plasma viscosity in isolated systolic hypertension: the role of pulse pressure, Am. J. Hypertens. 18 (7) (2005) 1005–1008.
[21] L.P. Katherine, Cytoarchitecture and physical properties of cytoplasm: volume, viscosity, diffusion, intracellular surface area [M], Microcompart. Phase Separ. Cytop. (1999) 189–221.
[22] H.P. Kao, J.R. Abney, A.S. Verkman, Determinants of the translational mobility of a small solute in cell cytoplasm, J. Cell Biol. 120 (1993) 175–184.
[23] M.M. Smith, P.C. Chen, C.S. Li, et al., Whole blood viscosity and microvascular abnormalities in Alzheimer's Disease, Clin. Hemorheol. Microcirc. 41 (4) (2009) 229–239.
[24] M.G. Ren, K. Zhou, L. Wang, et al., Construction of a ratiometric two-photon fluorescent probe to monitor the changes of mitochondrial viscosity, Sensor. Actuator. B Chem. 262 (2018) 452–459.
[25] S.J. Singer, G.L. Nicolson, The fluid mosaic model of the structure of cell membranes, Science 175 (1972) 720–731.
[26] E.O. Puchkov, Intracellular viscosity: methods of measurement and role in metabolism, Biochem. Suppl. Ser. A: Membr. Cell Biol. 7 (4) (2013) 270–279.
[27] S.Z. George, K. Ursula, S. Tomoyoshi, Platelet membrane fluidity individuals at risk for Alzheimer's disease- a comparison of results from fluorescence spectroscopy and electron spin resonance spectroscopy, Psychopharmacology 145 (1999) 175–180.
[28] Y.Y. Ma, Y.P. Zhao, R. Guo, et al., A near-infrared emission fluorescent probe with multi-rotatable moieties for highly sensitive detection of mitochondrial viscosity in an inflammatory cell model, J. Mater. Chem. B 6 (39) (2018) 6212–6216.
[29] Z. Yang, Y. He, J.H. Lee, et al., A self-calibrating bipartite viscosity sensor for mitochondria, J. Am. Chem. Soc. 135 (24) (2013) 9181–9185.
[30] S.C. Lee, J. Heo, H.C. Woo, et al., Fluorescent molecular rotors for viscosity sensors, Chemistry 24 (52) (2018) 13706–13718.
[31] Y.Y. Zhang, Z. Li, W. Hu, et al., A mitochondrial-targeting near-infrared fluorescent probe for visualizing and monitoring viscosity in live cells and tissues, Anal. Chem. 91 (15) (2019) 10302–10309.
[32] Z. Zou, Q. Yan, S.X. Ai, et al., Real-time visualizing mitophagy-specific viscosity dynamic by mitochondria-anchored molecular rotor, Anal. Chem. 91 (13) (2019) 8574–8581.
[33] H. Li, C.Q. Xin, G.B. Zhang, et al., A mitochondria-targeted two-photon fluorogenic probe for the dual-imaging of viscosity and H2O2 levels in Parkinson's disease models, J. Mater. Chem. B 7 (27) (2019) 4243–4251.
[34] Z.X. Tong, W. Liu, H. Huang, et al., A ratiometric fluorescent pH probe based on keto-enol tautomerization for imaging of living cells in extreme acidity, Analyst 142 (20) (2017) 3906–3912.
[35] G.P.C. Drummen, Fluorescent probes and fluorescence (microscopy) techniques–illuminating biological and biomedical research, Molecules 17 (12) (2012) 14067–14090.
[36] S. Wang, W.X. Ren, J.-T. Hou, et al., Fluorescence imaging of pathophysiological microenvironments, Chem. Soc. Rev. 50 (16) (2021) 8887–8902.
[37] M. Ren, Q. Xu, S. Wang, et al., A biotin-guided fluorescent probe for dual-mode imaging of viscosity in cancerous cells and tumor tissues, Chem. Commun. 56 (87) (2020) 13351–13354.
[38] W. Wang, Y. Liu, J. Niu, et al., Discriminating normal and inflammatory models by viscosity changes with a mitochondria-targetable fluorescent probe, Analyst 144 (21) (2019) 6247–6253.
[39] J. Yin, M. Peng, W. Lin, Visualization of mitochondrial viscosity in inflammation, fatty liver, and cancer living mice by a robust fluorescent probe, Anal. Chem. 91 (13) (2019) 8415–8421.
[40] R. Guo, J. Yin, Y. Ma, et al., A novel mitochondria-targeted rhodamine analogue for the detection of viscosity changes in living cells, zebra fish and living mice, J. Mater. Chem. B 6 (18) (2018) 2894–2900.